Chemical composition of PM$_{2.5}$ in an urban environment in Chengdu, China: Importance of springtime dust storms and biomass burning

Jun Tao [a,b,*], Leiming Zhang [b,c], Guenter Engling [d,**], Renjian Zhang [b], Yihong Yang [a], Junji Cao [e], Chongshu Zhu [e], Qiyuan Wang [e], Lei Luo [f]

[a] South China Institute of Environmental Sciences, Ministry of Environmental Protection, Guangzhou, China
[b] RCE-TEA, Institute of Atmospheric Physics, Chinese Academy of Sciences, Beijing, China
[c] Air Quality Research Division, Science Technology Branch, Environment Canada, Toronto, Canada
[d] Department of Biomedical Engineering and Environmental Sciences, National Tsing Hua University, Hsinchu, Taiwan
[e] Key Laboratory of Aerosol, SKLLQG, Institute of Earth Environment, Chinese Academy of Sciences, Xi'an, China
[f] Institute of Plateau Meteorology, China Meteorological Administration, Chengdu, China

ARTICLE INFO

ABSTRACT

Daily PM$_{2.5}$ samples were collected in Chengdu, a megacity in southwest China, for a period of one month in every season during 2009–2010. Mass concentrations of water-soluble inorganic ions, organic carbon (OC), elemental carbon (EC), levoglucosan (LG), water soluble organic carbon (WSOC), and elements were determined to identify the chemical characteristics and potential sources of PM$_{2.5}$. The data obtained in spring were discussed in detail to explore the impacts of dust storms and biomass burning on the chemical aerosol properties. The daily PM$_{2.5}$ mass concentrations ranged from 49.2 to 425.0 μg m^{-3} with an annual average of 165.1 ± 85.1 μg m^{-3}. The highest seasonal average of PM$_{2.5}$ concentrations was observed in the winter (225.5 ± 73.2 μg m^{-3}) and the lowest in the summer (113.5 ± 39.3 μg m^{-3}). Dust storm influence was observed only during the spring, while biomass burning activities occurred frequently in late spring and early summer. In the spring season, water-soluble ions, total carbonaceous aerosols, and the sum of the dominant elements (Al, Si, Ca, Ti, Fe, Mn, Zn, Pb, and Cu) accounted for 30.0 ± 9.3%, 38.6 ± 11.4%, and 6.2 ± 5.3%, respectively, of the total PM$_{2.5}$ mass. Crustal element levels evidently increased during the dust storm episode and LG, OC, WSOC, Cl$^-$ and K$^+$ concentrations increased by a factor of 2-7 during biomass burning episodes. Using the Positive Matrix Factorization (PMF) receptor model, four sources for spring aerosols were identified, including secondary sulfate and nitrate, motor vehicle emissions, soil dust, and biomass burning. The four sources were estimated to contribute 24.6%, 18.8%, 23.6% and 33.0%, respectively, to the total PM$_{2.5}$ mass.

1. Introduction

Fine particulate matter with aerodynamic diameters less than 2.5 μm (PM$_{2.5}$) has been found to adversely impact human health (Dockery and Pope, 1994; Laden et al., 2000; Samet et al., 2000; Pope and Dockery, 2006), visibility (Sisler and Malm, 2000; Lowenthal and Kumar, 2005; Pitchford et al., 2007; Watson, 2002), and climate change (Jacob and Winner, 2009). To address these impacts, chemical composition, sources/sinks, and formation mechanisms of PM$_{2.5}$ need to be understood at local, regional, and global scales (McMurry, 2000; Kaufman et al., 2002; Putaud, et al., 2004; Querol et al., 2004; Solomon et al., 2008). Numerous studies on various topics involving PM$_{2.5}$ have been conducted around the world (e.g., Chan, et al., 1999; Lee and Kang, 2001; Lin, 2002; Ho et al., 2003; Putaud, et al., 2004;

* Correspondence to: J Tao, South China Institute of Environmental Sciences, Ministry of Environmental Protection, Guangzhou, China.
** Corresponding author.
E-mail addresses: taojun@scies.org (J. Tao), guenter@mx.nthu.edu.tw (G. Engling).

Hueglin et al., 2005; Lonati et al., 2005). However, such studies in China were still limited and were mostly conducted in developed regions during the past decade, e.g., the Beijing metropolitan area, the Yangtze River Delta (YRD), and the Pearl River Delta (PRD) (He et al., 2001; Ye et al., 2003; Andreae et al., 2008; Hu et al., 2008; Yang et al., 2011).

Chengdu is one of the biggest cities in China with a population of more than 10 million, located in the Sichuan Basin of Southwest China. Air pollution is a serious problem in this city due to the special topography surrounding the city. For example, Longquan Mountain to the east and Qionglai Mountain to the west of the city can render dispersion of locally produced pollutants to be ineffective and cause high levels of pollution under certain weather conditions. To date, only a few studies have reported chemical speciation data for $PM_{2.5}$ in the Sichuan Basin (Wei et al., 1999; Cao et al., 2007; Zhao et al., 2010; Yang et al., 2012) and there has been no systematic investigation for the city of Chengdu. To fill this knowledge gap, chemically-resolved $PM_{2.5}$ data were obtained at an urban site in Chengdu for a period of one month in each season. Eight carbon fractions, nine water-soluble ions, water-soluble organic carbon (WSOC), levoglucosan (LG), and 25 elements were determined. While the data from all four seasons are briefly discussed in this study, the spring data are discussed in more detail focusing on the investigation of the impacts of spring dust storms and biomass burning on the chemical properties of $PM_{2.5}$.

Studies conducted in the northern regions of China suggested that dust storms and local biomass burning activities had significant impacts on the chemical speciation of $PM_{2.5}$ (Zhang et al., 2003a; Cao et al., 2005; Zhang et al., 2008; Chang et al., 2010; Zhang et al., 2012). There is evidence that dust storms from the Gobi desert and regions in central Asia can reach Chongqing (a neighboring city 270 km southeast of Chengdu), causing increased $PM_{2.5}$ loadings (Zhao et al., 2010). Vast areas of farmland are located adjacent to the west, north, and southwest of Chengdu city. Following the spring harvest, local agricultural wastes (e.g., rapeseed straw, wheat straw, and waste wood) are commonly burned to remove unwanted biomass, control pests, and increase soil fertility. Some of the plant residues are also utilized as fuel for cooking in the rural areas surrounding the city. Thus, both dust storms and biomass burning are expected to significantly aggravate the air quality of Chengdu. To complement our discussion, routinely monitored PM_{10} data were included in order to demonstrate the impact of dust storms in the spring season. In addition, three sets of $PM_{2.5}$ data obtained from near-source biomass burning measurements are presented for comparison with the ambient urban $PM_{2.5}$ data.

2. Methodology

2.1. Data collection

$PM_{2.5}$ samples were collected at the Institute of Plateau Meteorology (IPM), China Meteorological Administration, located in the urban area of Chengdu (30°39′43″N, 104°00′56″ E) (Fig. 1). The instruments used in this study were installed on the roof (15 m above ground) of an office building of the IPM. The site was surrounded by several streets with typical city traffic, representative of the urban environment in Chengdu.

The $PM_{2.5}$ samples were collected using two low-flow air samplers (MiniVol TAC, AirMetrics Corp., Eugene, OR, USA). Samples were collected at a flow rate of 5 L min^{-1} on two types of filters: 47 mm quartz fiber filters (Whatman QM-A) and 47 mm Teflon filters (Whatman PTFE). Quartz filters were pre-heated at 800 °C for 3 h prior to sampling. The exposed filters were stored in a freezer at −18 °C before chemical analysis to minimize the evaporation of volatile components. Teflon filters were analyzed gravimetrically for particle mass concentrations using a Sartorius MC5 electronic microbalance with a sensitivity of ±1 μg (Sartorius, Göttingen, Germany) after 24-h equilibration at a temperature between 20 °C and 23 °C and a relative humidity (RH) between 35% and 45%. Each filter was weighed at least three times before and after sampling, and the net mass was obtained by subtracting the average of the pre-sampling weights from the average of the post-sampling weights. Differences among replicate weightings were <10 μg for the blanks and <20 μg for the samples. Prior to the start of the sampling campaign, the flow rate of the $PM_{2.5}$ samplers was calibrated. Also, field blank filters were collected
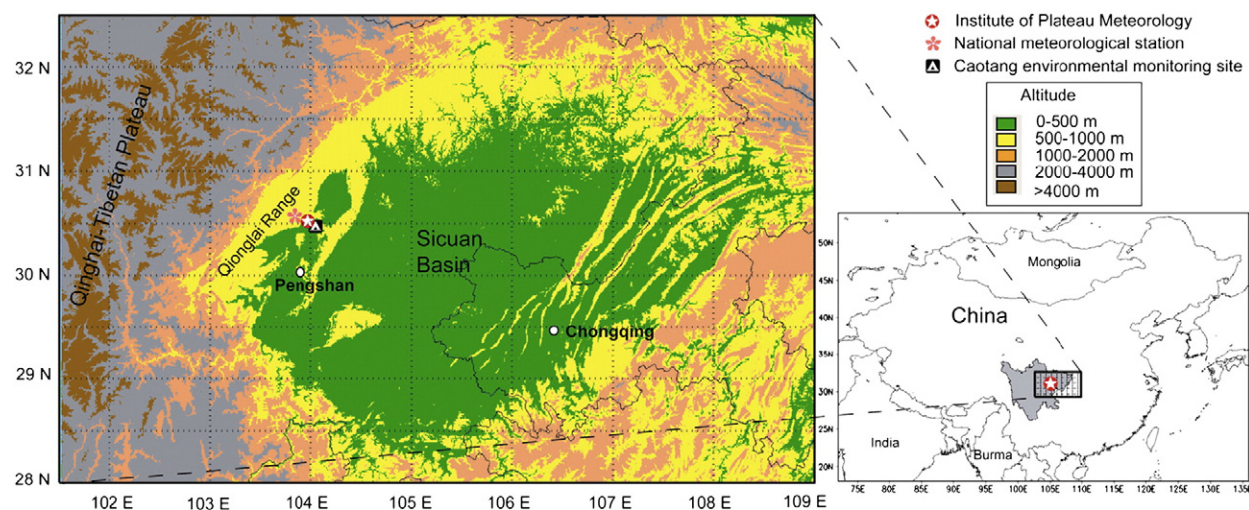

Fig. 1. Location of the sampling site in Chengdu, China.

and used to account for the positive artifacts caused by absorption of volatile organic compounds (VOCs) and to correct for background concentrations or influences from handling and transport.

A total of 121 $PM_{2.5}$ samples and 10 blank samples were collected during the periods of 19 April to 17 May (representative of spring), 6 July to 6 August (summer), 26 October to 26 November (autumn) in 2009, and 1 to 31 January (winter) in 2010. The collection duration for each sample was 24 h (starting at 10:00 local time each day and ending at 10:00 the next day).

Biomass burning smoke particle samples were collected in a wheat field in June, 2011 at Huangfeng town, Pengshan County, located 56 km south of Chengdu (30°10′N, 103°58′E) (Fig. 1). There was no obvious pollution source within a 10 km circle, and the air quality was in a good range (air pollutant index, API<50). A clear sky and calm wind conditions were also favorable for the collection of pure smoke emissions from the biomass burning near-source experiments. Three sets of $PM_{2.5}$ samples were collected within the biomass burning plumes by a low-flow air sampler (MiniVol TAC, AirMetrics Corp., Eugene, OR, USA) with a sampling duration for each source sample of 45 min in the afternoon on 7 June, 2011. Two sets of field blank samples were also collected, which were obtained by mounting the filters in the sampler for 15 min without airflow. The samplers were calibrated before sampling using a calibration orifice.

2.2. Chemical analysis of $PM_{2.5}$ filter samples

A 0.5 cm^2 punch from each quartz filter was analyzed for eight carbon fractions following the IMPROVE_A thermal/ optical reflectance (TOR) protocol on a DRI model 2001 carbon analyzer (Atmoslytic Inc., Calabasas, CA, USA) (Cao et al., 2003; Chow et al., 2007). This analysis produced four OC fractions (OC1, OC2, OC3, and OC4 at 140 °C, 280 °C, 480 °C, and 580 °C, respectively, in a helium [He] atmosphere); OP (a pyrolyzed carbon fraction determined when transmitted laser light attained its original intensity after oxygen [O_2] was added to the analysis atmosphere); and three EC fractions (EC1, EC2, and EC3 at 580 °C, 740 °C, and 840 °C, respectively, in a 2% O_2/98% He atmosphere). IMPROVE_TOR OC is operationally defined as OC1 + OC2 + OC3 + OC4 + OP and EC is defined as EC1 + EC2 + EC3 − OP (Chow et al., 2007). Inter-laboratory comparison of samples between IMPROVE_TOR protocol and the TMO (thermal manganese dioxide oxidation) approach has shown a difference of <5% for TC and <10% for OC and EC (Cao et al., 2003). Average field blanks had OC and EC contents of 1.82 and 0.10 μg m^{-3}, respectively, which were subtracted from each sample filter.

One-fourth of each quartz filter sample was used to determine the water-soluble ion concentrations. Four anions (SO_4^{2-}, NO_3^-, Cl$^-$, and F$^-$) and five cations (Na$^+$, NH_4^+, K$^+$, Mg^{2+}, and Ca^{2+}) were determined in aqueous extracts of the filters by ion chromatography (IC, Dionex DX-600, Dionex Corp., Sunnyvale, CA, USA). The extraction of water-soluble species from the quartz filters was achieved by placing the cut portion (1/4) of each filter into a separate 20 mL vial, followed by 10 mL distilled-deionized water (with a resistivity of >18 MΩ), and then subjected to ultrasonic agitation for 1 h, as well as additional shaking (using a mechanical shaker) for 1 h, for complete extraction of the ionic compounds. The extract solutions were filtered (0.25 μm, PTFE, Whatman, USA) and

stored at 4 °C in pre-cleaned tubes until analysis. Cation (Na$^+$, NH_4^+, K$^+$, Mg^{2+}, and Ca^{2+}) concentrations were determined by using a CS12A column (Dionex Corp.) with 20 mM MSA eluent. Anions (SO_4^{2-}, NO_3^-, Cl$^-$, and F$^-$) were separated on an AS11-HC column (Dionex Corp.), using 20 mM KOH as the eluent. A calibration was performed for each analytical sequence. The detection limits (DLs) of Na$^+$, NH_4^+, K$^+$, Mg^{2+}, Ca^{2+}, F$^-$, Cl$^-$, NO_3^-, and SO_4^{2-} were 0.0203, 0.0041, 0.0045, 0.0032, 0.0049, 0.0381, 0.0352, 0.1037 and 0.1094 μg m^{-3}, respectively. Standard reference materials (SRMs) obtained from the National Research Center for Certified Reference Materials, China, were analyzed for quality assurance purposes. Procedural blank values were subtracted from sample concentrations (Shen et al., 2009; Zhang et al., 2011).

A 2.0 cm^2 punch from each quartz filter was extracted in 15 mL of ultrapure water (Milli-Q Reference system) under ultrasonic agitation for 1 h for determination of water-soluble organic carbon (WSOC). The extracts were filtered through a syringe filter (0.25 μm, PTFE, Whatman, USA) to remove insoluble materials. WSOC was measured by a Sievers 900 TOC analyzer (GE Analytical, U.S.A.). The accuracy of the WSOC method for this data set, as determined by the average % recovery ± one standard deviation of standard mixtures of KHP (potassium hydrogen phthalate), was 107 ± 8%. All samples were corrected by laboratory blanks and subsequently by field blanks for WSOC contamination of filters, glassware, ultrapure water, etc. A calibration was performed for each analytical sequence. The DL of WSOC was 0.280 μg m^{-3}. An average blank concentration per filter area of 1.094 μg C m^{-3} was subtracted from each sample.

An additional portion of each filter (2.0 cm^2 punch) was extracted in 2 mL of ultrapure water under ultrasonic agitation for 1 h. The extracts were filtered through a syringe filter (0.25 μm, PTFE, Whatman, USA) to remove insoluble materials. The anhydrosugar levoglucosan was measured by a Dionex ICS-3000 system consisting of SP (quaternary pump), DC (column compartment), and ED (electrochemical detector with gold working electrode) (Dionex Corp., Sunnyvale, CA, USA). Instrumental controls, data acquisition, and chromatographic integration were performed using Dionex Chromeleon software. A calibration was performed for each analytical sequence. The DL for LG was 0.024 μg m^{-3}. A detailed description of the analytical method can be found in Engling et al. (2006) and Iinuma et al. (2009).

Specific elements were quantified using X-ray fluorescence analysis (XRF, Epsilon5, PANalytical Company, Netherlands) on Teflon filters, including sodium (Na), magnesium (Mg), aluminum (Al), silica (Si), phosphor (P), sulfur (S), chlorine (Cl), potassium (K), calcium (Ca), titanium (Ti), zinc (Zn), iron (Fe), lead (Pb), manganese (Mn), copper (Cu), vanadium (V), arsenic (As), tin (Sn), bromide (Br), rubidium (Rb), nickel (Ni), selenium (Se), chromium (Cr), cobalt (Co), and strontium (Sr). Quality Assurance/Quality Control (QA/QC) procedures of the XRF analysis procedure were described in Xu et al. (2012).

2.3. Data analysis methods

To identify source regions of dust storms reaching Chengdu, three-day backward trajectories at 02:00 UTC (10:00 local time) on every sampling day were calculated by the HYSPLIT 4 trajectory model (http://ready.arl.noaa.gov/HYSPLIT.php) to

demonstrate the synoptic patterns and associated long-range transport routes of air masses. The model adopts meteorological data from FNL (Final Operational Global Analysis) as the input. The aerosol index determined from TOMS on board of NASA's Earth Probe satellite (available at http://toms.gsfc.nasa.gov/) was used to obtain the geographical distribution of aerosols in the region of interest during the dust storm episode.

Source apportionment was conducted using EPA PMF 3.0 Model (Norris et al., 2008). The uncertainties for the LG and WSOC data were based on the standard deviation of repeated analysis of standard reference materials, field blanks, and instrumental detection limits. For the inorganic ions and carbon fractions detected in the blanks and samples, the uncertainty was calculated from the square root of the sum of the squares of the standard deviation of the blanks and the analytical uncertainty. The analytical uncertainty for each compound was calculated as the measured value times the relative uncertainty of the compound in the replicate measurements of the standard reference materials. The detected concentrations of the eight carbon fractions, eight water-soluble ions (except Mg^{2+}), water-soluble organic carbon (WSOC), and LG were larger than their respective DLs. However, only 10 (Al, Si, Ca, Ti, Fe, Cr, Mn, Zn, Pb, and Cu) out of the 25 elements had the average concentrations higher than the DLs. Therefore, we only used these 10 elements for the PMF analysis. For the 10 selected elements, four out of the 29 (or 13.8%) bulk $PM_{2.5}$ samples had Cr concentrations lower than its DL. Thus, we assumed 1/2 DL concentration and an uncertainty of 5/6 DL for Cr only for these four samples following the suggestion of Polissar et al. (1998). Based on the magnitudes of the concentrations of the chemical species determined, a total of 22 dominant species (OC, EC, Na^+, NH_4^+, K^+, Ca^{2+}, F^-, Cl^-, NO_3^-, SO_4^{2-}, WSOC, LG, Al, Si, Ca, Ti, Fe, Cr, Mn, Zn, Pb and Cu) were selected for the PMF analyses. To obtain source identification, 29 (samples) × 23 (chemical species) was input into the PMF model.

According to the IMPROVE equations, the dry $PM_{2.5}$ mass concentration can be reconstructed according to the IMPROVE Report V (2011):

$$[PM_{2.5}] = [(NH_4)_2SO_4] + [NH_4NO_3] + [POM] + [LAC] + [Soil]$$

where $[(NH_4)_2SO_4] = 1.375 [SO_4^{2-}]$, $[NH_4NO_3] = 1.29 [NO_3^-]$, [POM] is particulate organic matter ([POM] = 2.0 [OC]) (Chen and Yu, 2007; Andreae et al., 2008), [LAC] is light absorbing carbon, referred to as [EC], and [Soil] is soil concentration ([Soil] = 2.2 [Al] + 2.49 [Si] + 1.63 [Ca] + 2.42 [Fe] + 1.94 [Ti]).

3. Results and discussion

3.1. Overview of PM_{10} and $PM_{2.5}$ mass concentrations

To identify the occurrence of dust storms and gain a general knowledge of the PM levels in Chengdu city, PM_{10} data in 2009 are first briefly evaluated. Daily PM_{10} concentrations were available from the Caotang national environmental monitoring site (30°39′15″N, 104°01′43″E) (Fig. 1), located 1.5 km southeast of the IPM site. Meteorological data were obtained from a national meteorological station (30°42′N, 103°50′E) located 18 km away from IPM (Fig. 1). Monthly

average PM_{10} data and several meteorological parameters are shown in Fig. 2.

Clear seasonal variations in PM_{10} concentrations were observed throughout the year, with the lowest concentrations in the summer and the highest in the winter and fall. The low concentrations in the summer were likely due to the frequent rainfall since precipitation scavenging is an efficient way of removing particles from the atmosphere. In fact, 70% of the annual precipitation occurred during the three-month period from July to September. High PM_{10} concentrations in the winter and fall might be at least partly due to the lower mixing height and low wind speeds, both rendering dispersion of pollutants less effective. The daily PM mass data (figure not shown) revealed the highest concentration (668 μg m^{-3}) on 24 April, 2009. On this day, a dust storm event was observed across a large area of northern China (Wang et al., 2011). It is plausible that the same dust event also affected Chengdu. In comparison, the second highest daily concentration in Chengdu was only 372 μg m^{-3} on 18 January, 2009.

The $PM_{2.5}$ mass concentrations were derived from gravimetric analyses of 121 sample filters. The daily $PM_{2.5}$ mass concentrations ranged from 49.2 to 425.0 μg m^{-3} with an annual average of 165.1 ± 85.1 μg m^{-3}, exceeding the Chinese National Ambient Air Quality Standards (GB3095-2012) (35 μg m^{-3}) by a factor of ~4.7. This suggests that the $PM_{2.5}$ pollution at Chengdu was serious and control measures should be undertaken to alleviate the $PM_{2.5}$ loading. The seasonal patterns in $PM_{2.5}$ concentrations were similar to those of PM_{10}, with averages decreasing in the order of winter (225.5 ± 73.2 μg m^{-3}), autumn (188.0 ± 106.9 μg m^{-3}), spring (133.2 ± 55.5 μg m^{-3}), and summer (113.5 ± 39.3 μg m^{-3}). The spring $PM_{2.5}$ level in Chengdu was evidently higher than those in many other megacities in China, such as Beijing (88.6 μg m^{-3}) (He et al., 2001), Guangzhou (79.2 μg m^{-3}) (Tao et al., 2009), and Shanghai (61.7 μg m^{-3}) (Ye et al., 2003).

$PM_{2.5}$ mass concentrations were reconstructed in four seasons according to the IMPROVE equations presented in Section 2.3 (Fig. 3). The percentages of POM and Soil in $PM_{2.5}$ were 31.1% and 15.0%, respectively, in the spring, which were significantly higher than in any other season. The correlation between OC and EC in the spring was much lower ($R^2 = 0.32$) compared to other seasons ($R^2 = 0.69$–0.88) (Fig. 4). These results indicate that the sources for carbonaceous aerosols were more complex in the spring than in the other seasons, and that dust storms and biomass burning played more important roles during spring. Thus, in the following sections, the impacts of dust storms and biomass burning on $PM_{2.5}$ characteristics were investigated in detail and major sources contributing to spring $PM_{2.5}$ were explored using the Positive Matrix Factorization (PMF) method.

3.2. Identification of dust storm and biomass burning episodes in springtime

Crustal elements (Al, Si, Ca, Ti, and Fe) have been commonly used as source tracers of dust storm influence (Zhang et al., 2003b). The anhydrosugar levoglucosan (LG), derived from the thermal degradation of cellulose, has been widely used as a molecular source tracer of biomass burning emissions (Engling et al., 2006; Zhang et al., 2008, 2010; Kundu et al.,
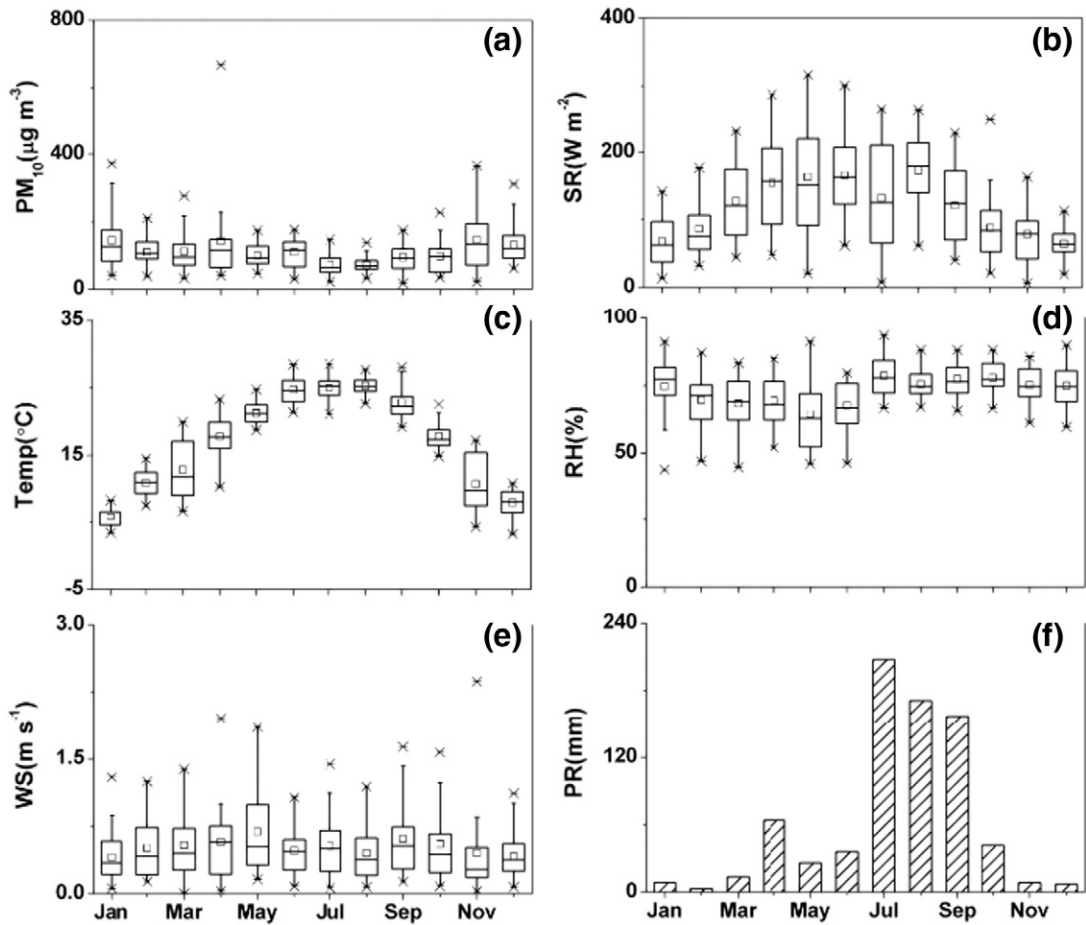
Fig. 2. Monthly average of (a) PM_{10}, (b) SR (solar radiation), (c) Temp (temperature), (d) RH (relative humidity), (e) WS (wind speed), and (f) PR (precipitation). A normal distribution is fitted to the measurements within each bin and minimum, 1st, 25th, 50th, 75th, 99th and maximum percentiles.
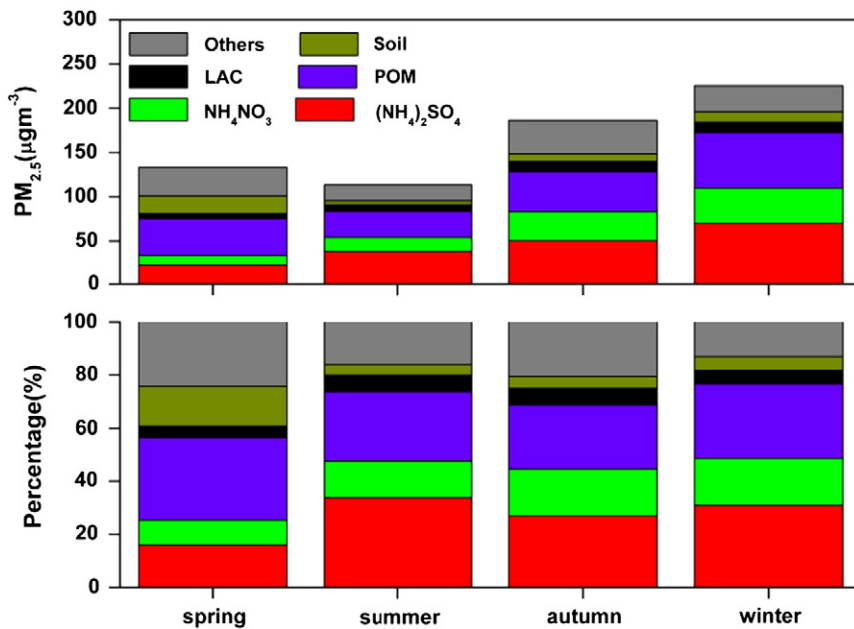

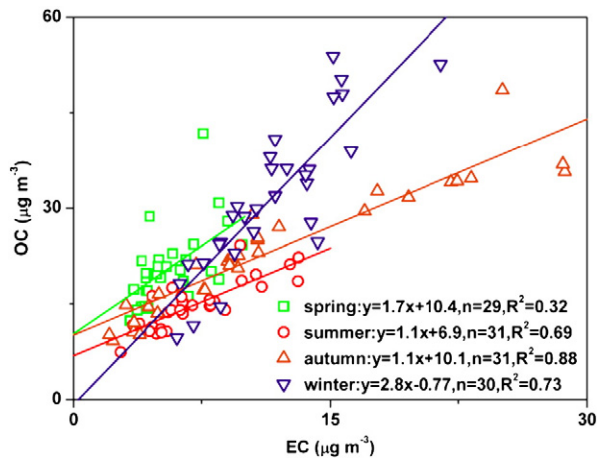**Fig. 3.** Reconstructed $PM_{2.5}$ mass concentrations in four seasons.

Fig. 4. Relationship between OC and EC in four seasons.

2010). During the observation period, one heavy dust storm (DS) episode and three biomass burning (BB) episodes were observed on 24–26 April (DS) (Wang et al., 2011), 5 May (BB1), 13 May (BB2), and 17 May (BB3), respectively (Table 1 and Fig. 5). The DS and BB events were defined as episodes when the respective tracer concentrations exceeded their average values plus one standard deviation, i.e., Al, Si, Ca, Ti, and Fe concentrations exceeded 6.5, 6.6, 4.3, 0.5 and 5.6 μg m^{-3}, respectively, and LG concentrations exceeded 801.8 ng m^{-3}. Non-episodic days (NED) were the remaining periods without DS and BB episodes.

The average $PM_{2.5}$ concentrations were 242.5 μg m^{-3} and 156.5 μg m^{-3} during DS and BB episodes, respectively, which were significantly higher than those during NED periods (115.8 μg m^{-3}). The elemental concentrations of Al, Si, Ca, Fe, and Ti were 13.0, 13.5, 8.13, 10.7, and 0.88 μg m^{-3}, respectively,

during the DS episode, which were evidently higher than those in the non-dust storm periods.

To investigate the origins and transport pathways of soil dusts, 72-h air mass back trajectories arriving at 500, 1000 and 1500 m above ground level on 24, 25 and 26 April were calculated for the IPM station using the NOAA HYSPLIT 4 trajectory model (Fig. 6). During the three dust days, air masses originated from the western part of Mongolia, moved along the northern boundary of Inner Mongolia, and passed through Gansu Province, before reaching IPM. This dust storm was identified as a serious sandstorm affecting large areas of northern China (Wang et al., 2011). The TOMS aerosol index revealed that dust aerosols over northwestern China extended from Mongolia to Inner Mongolia and Gansu Province on 24 April (Fig. 7a). The soil dust was transported to Chengdu by northerly airflow as well, causing $PM_{2.5}$ and PM_{10} concentrations as high as 300.5 μg m^{-3} and 668 μg m^{-3}, respectively, on 24 April. When dust aerosols spread eastward on 25 April (Fig. 7b), the impact of the dust storm became weaker and the $PM_{2.5}$ and PM_{10} levels decreased to 266.0 μg m^{-3} and 461 μg m^{-3}, respectively.

The average LG concentration was 1412.5 ng m^{-3} during the three BB episodes, five times higher than those during the NED periods (290.3 ng m^{-3}) and seven times higher than that during the DS episode (194.8 ng m^{-3}) (Table 1). High concentrations of LG were also measured in smoke particles produced by the burning of wheat straw and rape straw (Table 2).

Besides the one DS and three BB events, high $PM_{2.5}$ and LG concentrations were also observed on the 29th of April. The $PM_{2.5}$ concentration reached 216.7 μg m^{-3}, the second highest only next to the DS event period, and the LG concentration reached 508.8 ng m^{-3}, much higher than the average LG concentration (396.5 ng m^{-3}). Apparently, biomass burning had significant contributions to the $PM_{2.5}$ mass on this particular day. However, considering that the LG concentration on this day did not exceed 801.8 ng m^{-3}, we did not treat it as a

Table 1

Average concentrations of $PM_{2.5}$ and associated chemical components during the spring intensive campaign in Chengdu, China. DS, BB and NED represent dust storm, biomass burning, and non-episodic periods, respectively.

| Components	NED1	DS	NED2	BB1	NED3	BB2	NED4	BB3	NED	DS	BB	Ave.
	19–23 April	24–26 April	27 April–4 May	5 May	6–12 May	13 May	14–16 May	17 May				
$PM_{2.5}$ (μg·m^{-3})	107.8	242.5	130.1	189.2	119.1	118.5	83.5	161.8	115.8	242.5	156.5	133.2
LG (ng·m^{-3})	93.2	194.8	272.2	897.5	466.7	1820.9	255.2	1519.1	290.3	194.8	1412.5	396.5
OC (μg·m^{-3})	16.8	20.4	18.8	27.9	21.6	28.7	18.6	41.8	19.2	20.4	32.8	20.7
WSOC (μg·m^{-3})	8.2	9.9	9.3	15.5	10.6	17.4	9.5	21.4	9.5	9.9	18.1	10.4
EC (μg·m^{-3})	4.8	5.1	6.3	9.0	5.6	4.5	4.7	7.6	5.6	5.1	7.0	5.7
OC/EC	3.6	4.1	3.2	3.1	4.1	6.4	3.9	5.5	3.6	4.1	5.0	3.8
WSOC/OC	0.49	0.48	0.50	0.55	0.50	0.61	0.51	0.51	0.50	0.48	0.56	0.50
F^- (μg·m^{-3})	0.4	0.5	0.3	0.3	0.3	0.3	0.3	0.3	0.3	0.5	0.3	0.3
Cl^- (μg·m^{-3})	1.4	3.0	2.4	6.9	2.6	6.0	2.0	6.8	2.2	3.0	6.5	2.7
NO_3^- (μg·m^{-3})	6.4	5.7	13.0	21.4	9.3	6.1	8.6	9.5	9.9	5.7	12.3	9.7
SO_4^{2-} (μg·m^{-3})	12.4	12.6	18.7	32.6	16.9	8.9	8.6	14.0	15.4	12.6	18.5	15.5
Na^+ (μg·m^{-3})	0.9	1.7	0.3	0.0	0.3	0.3	0.1	0.6	0.4	1.7	0.3	0.5
NH_4^+ (μg·m^{-3})	2.1	0.7	6.7	13.4	5.6	3.5	2.4	5.4	4.8	0.7	7.4	4.6
K^+ (μg·m^{-3})	1.3	1.9	2.8	4.3	3.7	6.4	2.3	8.6	2.7	1.9	6.4	3.0
Mg^{2+} (μg·m^{-3})	0.0	0.3	0.0	0.0	0.0	0.0	0.0	0.0	0.0	0.3	0.0	0.0
Ca^{2+} (μg·m^{-3})	3.2	7.3	1.5	2.4	1.3	1.6	1.9	2.2	1.8	7.3	2.1	2.4
Al (μg·m^{-3})	2.60	13.0	1.24	0.73	0.75	0.29	0.32	0.62	1.27	13.0	0.55	2.41
Si (μg·m^{-3})	1.90	13.5	1.10	0.81	0.65	0.25	0.39	0.53	1.05	13.5	0.53	2.28
Ca (μg·m^{-3})	2.10	8.13	0.92	0.62	0.70	0.26	0.36	0.53	1.04	8.13	0.47	1.72
Fe (μg·m^{-3})	2.30	10.7	1.55	1.32	1.28	0.56	0.46	0.84	1.49	10.7	0.91	2.39
Ti (μg·m^{-3})	0.20	0.88	0.13	0.09	0.09	0.04	0.05	0.07	0.12	0.88	0.07	0.19
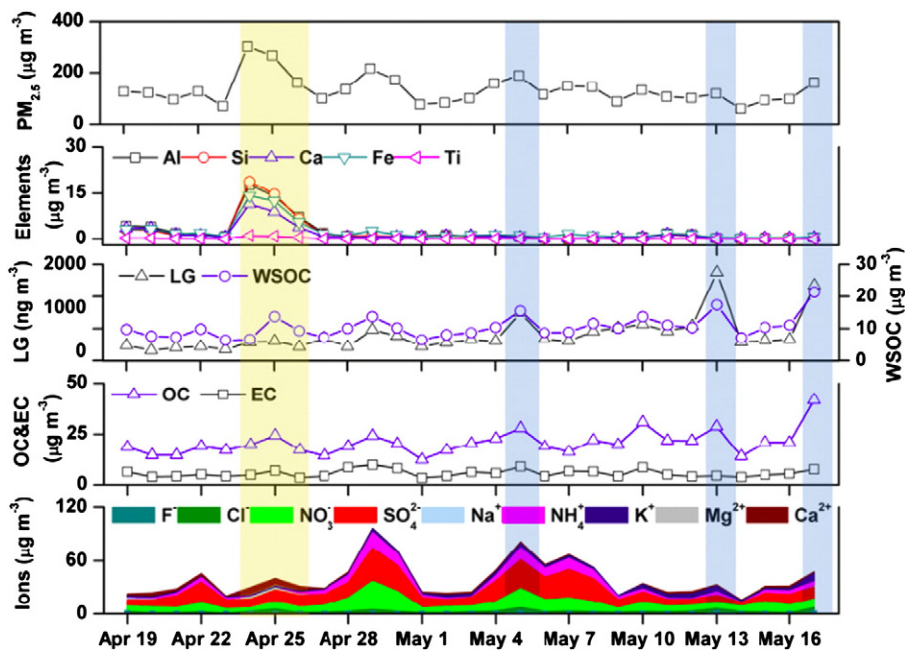
Fig. 5. Daily variations of PM$_{2.5}$ mass and its chemical species between 19 April and 17 May, 2009.

BB episode. On the other hand, the sulfate and nitrate concentrations on this day reached 37.2 µg m^{-3} and 31.7 µg m^{-3}, respectively, which were the highest levels during the whole spring period. These observations suggest that both secondary aerosols and biomass burning contributed to the higher PM$_{2.5}$ mass on this day. The calm weather (wind speeds <0.2 m s^{-1}) during the consecutive two days from 28 to 29 April was likely the main meteorological reason for the higher PM$_{2.5}$ concentrations.

3.3. Chemical composition of PM$_{2.5}$ during dust storm and biomass burning episodes

3.3.1. Ionic species

The sum of all the detected water-soluble ions was 39.2 ± 19.8 µg m^{-3} during the spring period, accounting for 30.0 ±

9.3% of the PM$_{2.5}$ mass. The average concentrations of the four anions followed the sequence of $SO_4^{2-} > NO_3^- > Cl^- > F^-$ while the five cations followed the order of $NH_4^+ > K^+ > Ca^{2+} > Na^+ > Mg^{2+}$. Sulfate, nitrate and ammonium dominated the water-soluble inorganic species, accounting for 72.9 ± 12.8% of the total ion concentration.

The average concentrations of Cl$^-$ and K$^+$ were 6.5 µg m^{-3} and 6.4 µg m^{-3}, respectively, during the BB period, which were substantially higher than those during the NED and DS periods. Good correlations between LG and Cl$^-$ and between LG and K$^+$ were found, suggesting that the excess Cl$^-$ and K$^+$ could be attributed to biomass burning emissions (Fig. 8). Similar results were also obtained by Ryu et al. (2004) and Hays et al. (2005). Moreover, high emission factors of Cl$^-$ and K$^+$ from rape straw and wheat straw burning also indicated that biomass burning affected the ambient levels of these ions
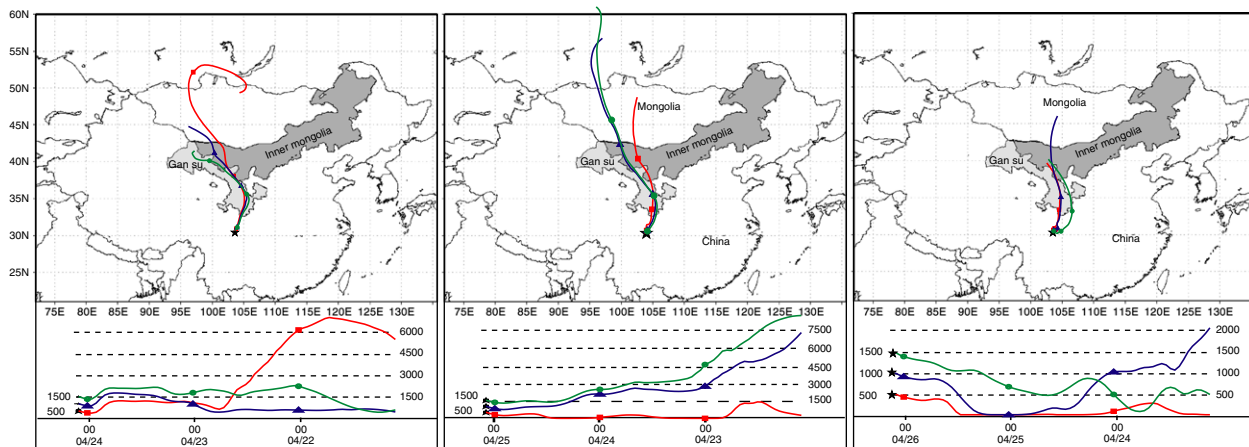

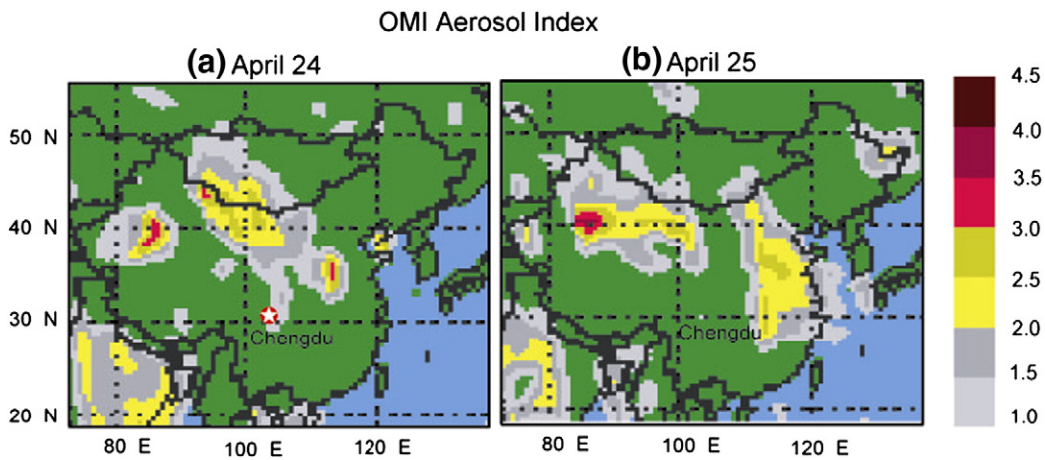**Fig. 6.** 72-h air mass back-trajectory analysis for dust storm days.

OMI Aerosol Index

Fig. 7. Aerosol index (AI) on 24 April (a) and 25 April (b). The "green" and "light blue" represent AI of land <1.0 and AI of ocean <1.0, respectively (Mahowald and Dufresne, 2004).

(Table 2). These findings were also consistent with those from previous studies (Hays et al., 2005; Engling et al., 2009; Kundu et al., 2010; Ram and Sarin, 2011). Although the Cl⁻ and K⁺ concentrations from wheat straw burning (flaming or smoldering) were higher than those from rape straw burning (flaming) (Table 2), the K⁺/PM$_{2.5}$ and Cl⁻/PM$_{2.5}$ ratios in rape straw smoke particles were actually much higher. This was likely due to the more complete combustion of rape straw. Another possible explanation could be a higher content of Cl⁻

Table 2
Dominant chemical components of PM$_{2.5}$ ($\mu g \cdot m^{-3}$) in smoke emissions from rape and wheat straw burning.

	Rape straw (flaming)	Wheat straw (flaming)	Wheat straw (smoldering)
PM$_{2.5}$	2537.5	8645.0	16,234.9
LG	30.4	264.0	389.4
OC	785.3	3857.1	7636.1
EC	347.8	239.7	460.1
OC1	65.2	1066.3	2442.4
OC2	162.1	1134.2	2386.0
OC3	204.6	769.0	1272.5
OC4	322.3	83.2	139.3
OP	31.2	804.4	1395.9
EC1	379.0	1042.9	1833.8
EC2	0.0	1.1	11.3
EC3	0.0	0.0	10.8
WSOC	335.2	1091.5	1636.2
F⁻	0.0	10.9	16.0
Cl⁻	257.5	475.2	999.3
NO$_3^-$	24.2	23.9	14.2
SO$_4^{2-}$	113.5	84.0	178.7
Na⁺	39.6	20.0	23.8
NH$_4^+$	0.5	54.7	72.3
K⁺	295.0	363.9	927.2
Mg^{2+}	0.0	9.3	5.8
Ca^{2+}	0.0	23.4	3.7
LG/PM$_{2.5}$ (%)	1.2	3.1	2.4
OC/PM$_{2.5}$ (%)	30.9	44.6	47.0
EC/PM$_{2.5}$ (%)	13.7	2.8	2.8
Cl⁻/PM$_{2.5}$ (%)	10.1	5.5	6.2
K⁺/PM$_{2.5}$ (%)	11.6	4.2	5.7
OC/EC	2.3	16.1	16.6
LG/OC	0.039	0.068	0.051
WSOC/OC	0.43	0.28	0.21

and K⁺ in rape straw, although this cannot be confirmed with the present data set.

Ca^{2+}, Mg^{2+} and Na⁺ concentrations were distinctly higher during the DS event than the NED period and BB episodes, which was apparently due to the large content of soil dust in the ambient aerosol particles during the DS periods (Shen et al., 2009).

Ion balance calculations are commonly used to evaluate the acid–base balance of aerosol particles. To calculate the cation/anion balance of PM$_{2.5}$, we converted the ion mass concentrations into microequivalents. The cation and anion microequivalents of fine particles were calculated as follows:

$$C \text{ (cation microequivalents m}^{-3}) = Na^+/23 + NH_4^+/18 + K^+/39 + Mg^{2+}/12 + Ca^{2+}/20 \quad (1)$$

$$A \text{ (anion microequivalents m}^{-3}) = F^-/19 + Cl^-/35.5 + NO_3^-/62 + SO_4^{2-}/48 \quad (2)$$

Strong correlations between anion and cation equivalents were found for all of the PM$_{2.5}$ samples (Fig. 9). Most samples had an anion/cation (A/C) ratio slightly higher than 1.0 during the NED and BB periods, indicating the acidic nature of the particles. On the other hand, the A/C ratios were lower than 1.0 during the DS period, indicating a deficiency in anions in the DS samples. The A/C ratio was 0.6 on 24 April and was slightly lower than 1.0 in the other two DS samples. The DS data indicated an apparent deficit of anions, which was probably due to the lacking measurement of carbonate (CO$_3^{2-}$) (Cao et al., 2005; Shen et al., 2007). The weak correlation between Ca^{2+} and SO$_4^{2-}$ concentrations found here further revealed that calcite was the major form of CO$_3^{2-}$ in the aerosol at Chengdu. The molar concentration of CO$_3^{2-}$ can be calculated as the deficit values of measured anions, and the CO$_3^{2-}$ concentration was then determined by multiplying the molar concentration values by 30 (Shen et al., 2007). A good correlation was observed between the measured and estimated CO$_3^{2-}$ in Asian dust samples in previous studies (Shen et al., 2007, 2009). According to this method, the average carbonate mass fraction calculated here
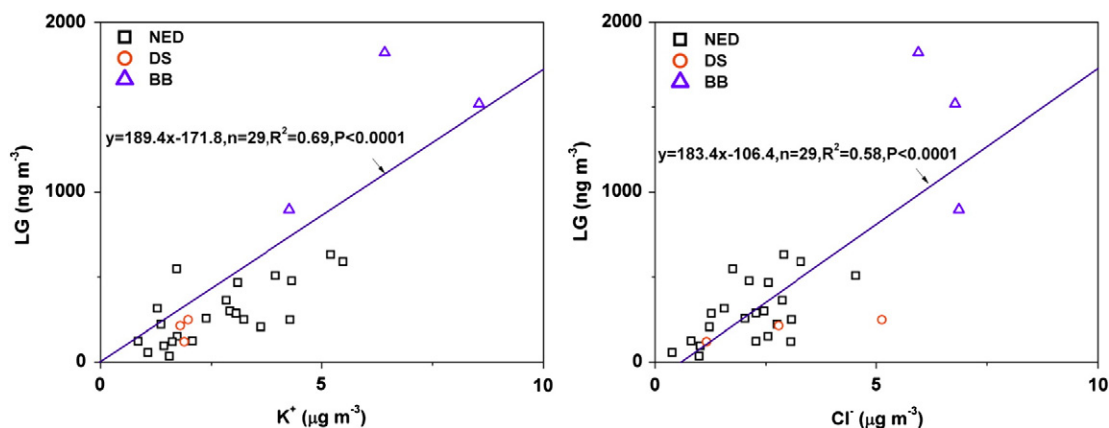
Fig. 8. Relationships between LG and K^+ and between LG and Cl^-.

was 2.6 µg m^{-3} during the DS episode, or 1.0% of PM$_{2.5}$, which was lower than those obtained in previous studies (Xu et al., 2004; Cao et al., 2005; Shen et al., 2009). It is noteworthy that Ca^{2+} maintained a high level over the following two days, while the A/C ratio was close to 1.0. This indicated that the abundant acidic compounds associated with urban pollution (i.e., SO_4^{2-} and NO_3^-) can react with the alkaline mineral dust components, leading to the loss of CO_3^{2-} and formation of $CaSO_4$, $MgSO_4$, $Mg(NO_3)_2$, or $Ca(NO_3)_2$ (Maxwell-Meier et al., 2004).

3.3.2. Carbonaceous species

The average OC, EC, and WSOC concentrations in PM$_{2.5}$ were 20.7 ± 6.0 µg m^{-3}, 5.7 ± 1.8 µg m^{-3} and 10.4 ± 3.4 µg m^{-3}, respectively, in the spring (Table 1). The POM and EC concentrations attributed 34.1 ± 10.6% and 4.5 ± 1.2%, respectively, of the PM$_{2.5}$ mass, while the total carbonaceous aerosol (POM + EC) accounted for 38.6 ± 11.4% of PM$_{2.5}$.

The average OC and WSOC concentrations were 32.8 µg m^{-3} and 18.1 µg m^{-3}, respectively, during the BB periods, which were substantially higher than those in the NED and DS periods. Good correlation between LG and OC and between LG and WSOC were found (Fig. 10), suggesting that significant amounts of OC and WSOC in ambient aerosols were associated

Fig. 9. Scatter plot of total cation microequivalents versus total anion microequivalents.

with biomass burning emissions (Kundu et al., 2010; Ram and Sarin, 2011). The chemical characteristics of smoke aerosol derived from commonly burned local biomass species (Table 2) also showed high OC and WSOC content. Moreover, slightly higher EC levels during the BB periods were likely due to incomplete combustion of biomass (Schwarz et al., 2008).

The sources of carbonaceous aerosols can be qualitatively evaluated with the relationship between OC and EC concentrations (Turpin and Huntzicker, 1995; Cao et al., 2007; Zhang et al., 2007). As shown in Fig. 4, the correlation between OC and EC in the spring was poor ($R^2 = 0.32$), which suggested that OC and EC were derived from different sources, i.e., emissions from traffic, coal combustion, and biomass burning. Watson et al. (2001) reported OC/EC ratios for coal combustion, vehicle emissions, and biomass burning with values of 2.7, 1.1, and 9.0, respectively. A recent examination of OC/EC ratios for different biomass burning sources revealed a wide range of values from 0.005 to 111, depending on the type of biomass (Minguillón et al., 2011). However, agricultural biomass burning was typically characterized by higher OC/EC ratios (>3.0) in Asia (Ryu et al., 2007; Engling et al., 2009, 2012). In this campaign, the average OC/EC ratio was 3.8 during the spring, indicating that biomass burning emissions indeed played an important role in particulate carbonaceous pollution in Chengdu. The average OC/EC ratio during the BB periods (5.0) was slightly higher than those during the DS (4.1) and ND (3.6) periods as expected. The OC/EC ratios for wheat straw and rape straw smoke aerosols were 16.4 and 2.3 (Table 2), respectively, supporting that the higher ambient OC/EC ratios were associated with wheat straw burning. The values for traffic emissions reported by Chirico et al. (2011) showed organic aerosol/black carbon (OA/BC) ratios, which are somewhat different from typical OC/EC ratios, yet provide additional information about carbonaceous aerosol characteristics from fossil fuel combustion (i.e., vehicle emissions), with characteristically low values of 1.0 or lower.

The average LG/OC ratio was 0.043 during the BB period, evidently higher than those in the DS (0.010) and NED (0.015) periods. The LG/OC ratios in ambient aerosols during the BB period were close to the ratios of those measured in rape straw and wheat straw near-source smoke particles, ranging from 0.039 to 0.068 (Table 2). The LG/OC ratio in rape straw was similar to those found in Hickory (0.037) and saw
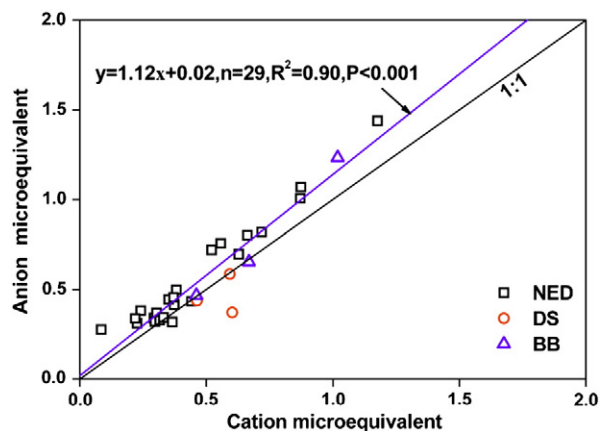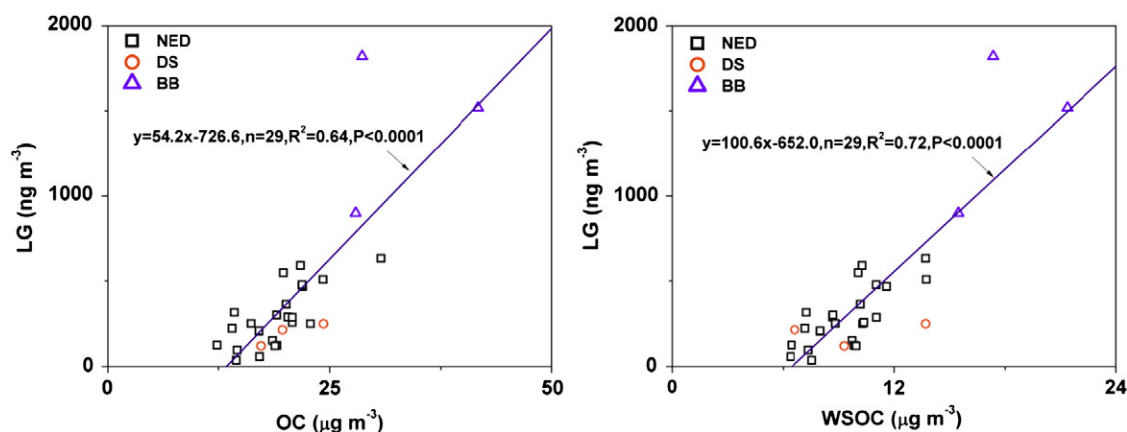
Fig. 10. Relationships between LG and OC as well as EC.

grass (0.041) (Sullivan et al., 2008). Moreover, the LG/OC ratio in wheat straw was similar to wax myrtle, titi, ponderosa pine duff, oak, fresh lodgepole pine, ceanothus and chamise (Sullivan et al., 2008) and to rice straw (Engling et al., 2012).

The average WSOC/OC ratio was 0.56 during the BB period, slightly higher than those in the DS (0.48) and NED (0.50) periods. Higher WSOC/OC ratios in ambient fine particles have been associated with biomass burning in previous studies as well (Kumagai et al., 2009; Rengarajan et al., 2011). However, the WSOC/OC ratios in rape straw and wheat straw near-source smoke particles ranged from 0.21 to 0.43, which were lower than the ratios in the ambient aerosol at Chengdu. Lower WSOC/OC ratios were also found in smoke particles derived from certain softwood, hard wood and grass species (Iinuma et al., 2007). The above results suggest that, while biomass burning could have increased the WSOC/OC ratios in ambient aerosols, the newly-emitted aerosols would have lower ratios compared to the slightly aged aerosols (noting that most previous studies collected aerosols at some distances away from the sources while the present study collected right above the sources). The most likely explanation is the formation of WSOC via atmospheric oxidation of the gaseous precursor species originating from biomass burning sources, resulting in more oxygenated secondary organic aerosol (SOA) species (Hennigan et al., 2011, 2012; Kondo et al., 2007). In addition, the particulate phase oxidation of organic compounds during atmospheric transport can be an important pathway for the formation of WSOC (Robinson et al., 2007).

3.3.3. Crustal elements

The crustal element Al, Si, Ca, Fe and Ti concentrations were evidently enhanced during the DS periods compared to the non-dust storm periods. The enrichment factors (EFs) relative to the earth upper crust can be used to compare the elemental composition of aerosol samples with those of crustal materials (Taylor and McLennan, 1995). The method is often applied to identify whether the elements have natural or anthropogenic origins. The EFs of $PM_{2.5}$ particles can be calculated as follows:

$$EFs = (C_{element}/C_{reference})_{aerosol}/(C_{element}/C_{reference})_{crust}$$

where $C_{element}$ and $C_{reference}$ are the concentrations of focused and reference elements, respectively.

Gao et al. (1992) suggested that Al, Fe, Sc, and Ba were commonly used as reference elements. Considering the many cement and steel factories in the suburban parts of Chengdu, we excluded Fe and Si as reference elements. On the other hand, few industrial factories emitted Al in the Chengdu area. Therefore, Al was used as the reference element based on the chemical composition of typical earth crust matter (Wedepohl, 1995). The enrichment factors of the five crustal elements were lower than 10 during the DS episode, as shown in Fig. 11, implying that these five elements were derived from crustal material rather than from anthropogenic sources (Veysseyre et al., 2001). EFs of Si were mostly as low as ~0.2, which were evidently lower than those reported in previous studies (Na and Cocker, 2009; Zhao et al., 2010). Compared with the crustal element data in Chongqing located 270 km east of Chengdu (Zhao et al., 2010), the average crustal element concentrations were similar to the crustal element concentrations (except Al) in this study. The higher Al concentration resulted in lower EFs of Si. Zhang et al. (2002) also found the EFs of Si were ~0.20 and ~0.39 in fine and coarse-mode particles, respectively, in Beijing. Moreover, the daily concentration variations of the five crustal elements were very similar and the EFs were lower than 10, which suggested that they were derived from the same source, i.e., crustal material in this study.

3.4. Source apportionment of $PM_{2.5}$

The Positive Matrix Factorization (PMF) model was used to identify $PM_{2.5}$ sources and estimate source contributions. For the determination of the number of sources, a reasonable practice is to test different numbers of sources commonly used and reference to those listed by the local Environmental Protection Bureau. The combinations of source types best fit to the measurement data and with the best physical meaning can then be chosen. In this study, we tested four, five and six different sources for the PMF analysis. After comparing the plots of Q values versus the number of sources, we found that the Q value with four sources is most consistent with the number of all the species (Reff et al., 2007). In addition, the four-source solution explains >95% of the variability in the data set, satisfying the criterion suggested by a PMF evaluation
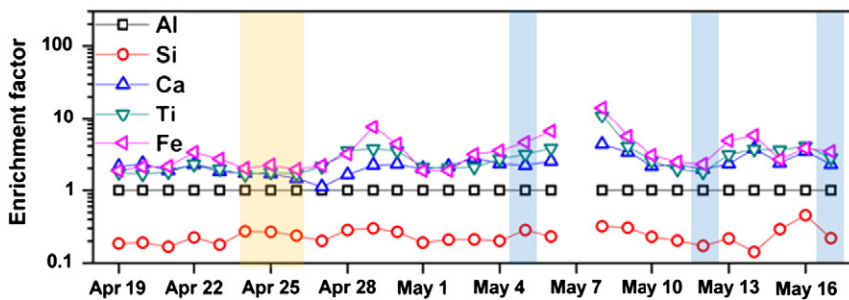
Fig. 11. Enrichment factors of crustal elements.

study (Chen et al., 2010). Therefore, we chose four sources as our final results. They were (1) secondary sulfate/nitrate, (2) motor vehicles and road dust, (3) soil dust and others, and (4) biomass burning.

The percentage loading from each chemical species to each factor (source type) is shown in Fig. 12. The time series of contributions from the 'soil dust and others' factor and from the 'biomass burning' factor are shown in Fig. 13. Clearly, soil dust contributions peaked during the identified dust storm period and biomass burning contributions were highest during the identified biomass burning episodes. The presence of secondary sulfate/nitrate was identified by high sulfate, nitrate and ammonium concentrations. These secondary products were formed from the oxidation of SO_2 and NO_x, which were emitted from traffic in the urban area and a power plant about 20 km away from the measurement site. Moreover, relatively high Cr and Pb concentrations suggested

the influence of coal combustion emissions which also constituted the main source of SO_2. The contribution of secondary sulfate and nitrate to the total $PM_{2.5}$ was 24.6% on average. Motor vehicle emissions were characterized by high OC, EC, and road dust components (Na^+, Ca^{2+} and Cr), which are typical for urban environments. The PM mass contribution of this factor was 18.8%. The source of soil dust was identified by the abundance of crustal elements, e.g., Al, Si, Ca, Fe and Ti. The mass contribution of the soil dust factor was 23.6%. Biomass burning processes were characterized by high LG, K^+, Cl^-, OC, EC, and WSOC content, which were also found in typical local source profiles (Table 2). High levels of LG, K^+, Cl^-, OC and WSOC indicated that biomass burning occurred frequently during the spring. Biomass burning processes were estimated to have contributed 33.0% to the $PM_{2.5}$ mass during the spring measurement period, consistent with the observed influence of smoke emissions from
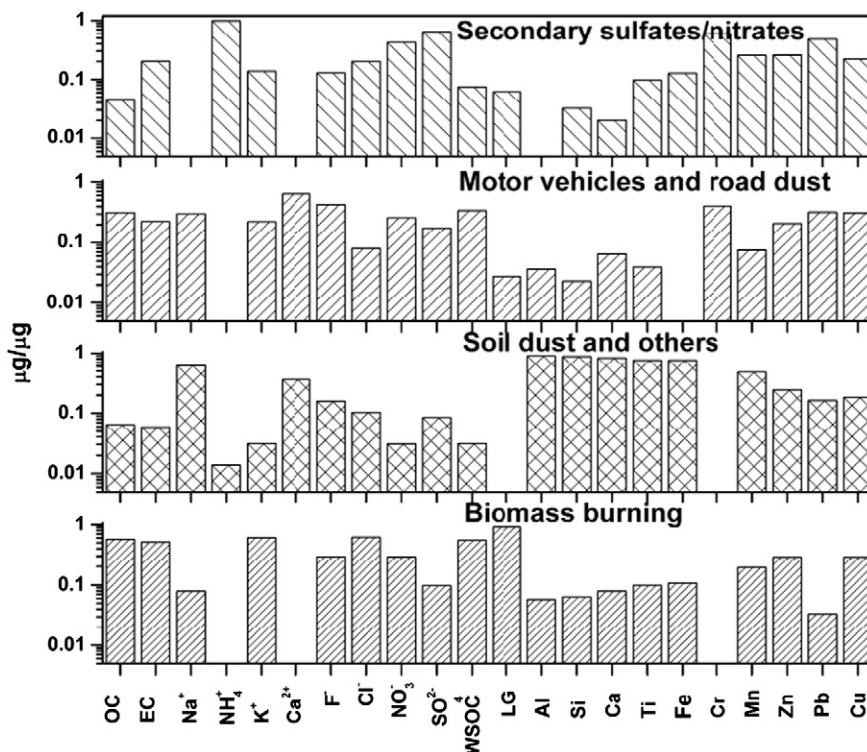

Fig. 12. Source profiles resolved from $PM_{2.5}$ samples for secondary sulfates/nitrates, motor vehicles and road dust, soil dust and others, and biomass burning in spring.
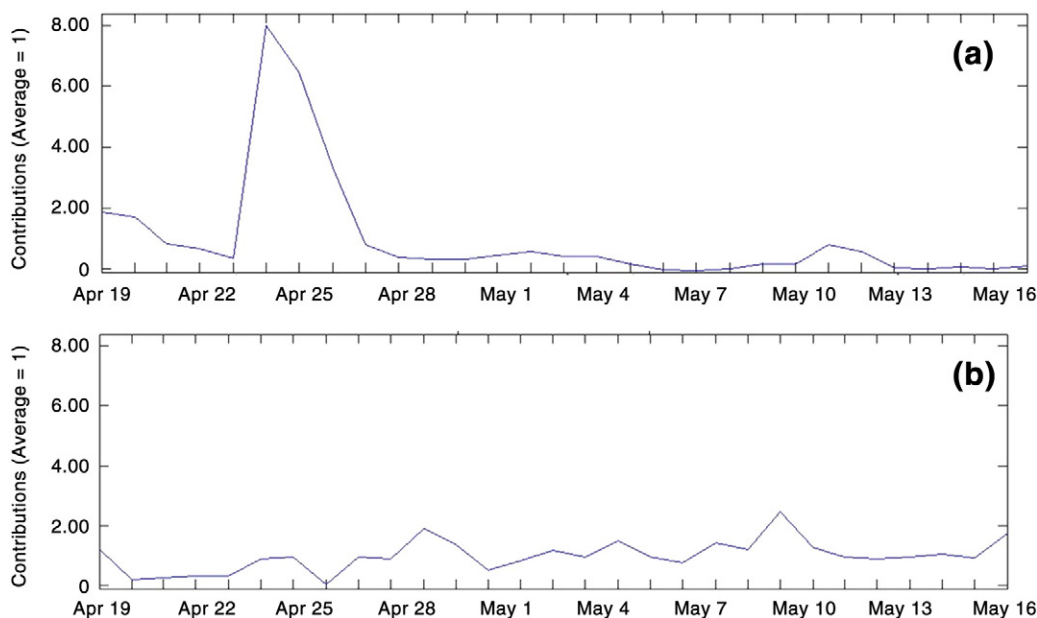
Fig. 13. The time series of contributions from (a) 'soil dust and others' factor, and (b) 'biomass burning' factor.

wheat straw, rape straw and other biomass fuel combustion throughout the suburban area.

4. Conclusions

Fine particulate matter and its chemical components in a megacity in southwest China were investigated in this study. $PM_{2.5}$ levels were high in all of the seasons and the annual average exceeded the Chinese National Ambient Air Quality Standards by nearly a factor of five. During the measurement periods (one month in every season between April 2009 and January 2010), one dust storm and three biomass burning episodes were identified in the late spring of 2009. Crustal element (Al, Si, Ca, Ti, and Fe) concentrations markedly increased during the dust storm episode. Elevated concentrations of LG, OC, WSOC, K^+ and Cl^- were found in ambient $PM_{2.5}$ during the biomass burning episodes and were also measured in large quantities in wheat straw and rape straw smoke particles obtained in a near-source combustion experiment. While the frequency of dust storm events in Chengdu was not as high as those in many northern cities of China, biomass burning activities in late spring and early summer seem to be a very important factor affecting $PM_{2.5}$ mass concentration and its chemical composition in this city. These findings filled critical knowledge gaps regarding $PM_{2.5}$ sources and composition in this region and provide scientific indication for the need of emission control policies yet to be developed in order to reduce $PM_{2.5}$ levels and thus human and environmental health impacts.

Acknowledgments

References

Andreae, M.O., Schmid, O., Yang, H., Chand, D., Yu, J.Z., Zeng, L.M., Zhang, Y.H., 2008. Optical properties and chemical composition of the atmospheric aerosol in urban Guangzhou, China. Atmos. Environ. 42, 6335–6350.

Cao, J.J., Lee, S.C., Ho, K.F., Zhang, X.Y., Zou, S.C., Fung, K., Chow, J.C., Watson, J.G., 2003. Characteristics of carbonaceous aerosol in Pearl River Delta Region, China during 2001 winter period. Atmos. Environ. 37, 1451–1460.

Cao, J.J., Lee, S.C., Zhang, X.Y., Chow, J.C., An, Z.S., Ho, K.F., Watson, J.G., Fung, K., Wang, Y.Q., Shen, Z.X., 2005. Characterization of airborne carbonate over a site near Asian dust source regions during spring 2002 and its climatic and environmental significance. J. Geophys. Res. 110, D03203. http://dx.doi.org/10.1029/2004JD005244.

Cao, J.J., Lee, S.C., Chow, J.C., Watson, J.G., Ho, K.F., Zhang, R.J., Jin, Z.D., Shen, Z.X., Chen, G.C., Kang, Y.M., Zou, S.C., Zhang, L.Z., Qi, S.H., Dai, M.H., Cheng, Y., Hu, K., 2007. Spatial and seasonal distributions of carbonaceous aerosols over China. J. Geophys. Res. 112, D22S11. http://dx.doi.org/10.1029/2006JD008205.

Chan, Y.C., Simpson, R.W., Mctainsh, G.H., Vowles, P.D., Cohen, D.D., Bailey, G.M., 1999. Source apportionment of visibility degradation problems in Brisbane (Australia) using the multiple linear regression techniques. Atmos. Environ. 33, 3237–3250.

Chang, S.C., Chou, C.C.K., Chen, W.N., Lee, C.T., 2010. Asian dust and pollution transport—a comprehensive observation in the downwind Taiwan in 2006. Atmos. Res. 95, 19–31.

Chen, X., Yu, J.Z., 2007. Measurement of organic mass to organic carbon ratio in ambient aerosol samples using a gravimetric technique in combination with chemical analysis. Atmos. Environ. 41 (39), 8858–8864.

Chen, L.-W.A., Lowenthal, D.H., Watson, J.G., Koracin, D., Kumar, N., Knipping, E.M., Wheeler, N., Craig, K., Reid, S., 2010. Toward effective source apportionment using positive matrix factorization: experiments with simulated $PM_{2.5}$ data. J. Air Waste Manag. Assoc. 60 (1), 43–54.

Chirico, R., Prevot, A.S.H., DeCarlo, P.F., Heringa, M.F., Richter, R., Weingartner, E., Baltensperger, U., 2011. Aerosol and trace gas vehicle emission factors measured in a tunnel using an Aerosol Mass Spectrometer and other on-line instrumentation. Atmos. Environ. 45, 2182–2192.

Chow, J.C., Watson, J.G., Chen, L.W., Chang, M.C., Robinson, N.F., Trimble, D., Kohl, S., 2007. The IMPROVE_A temperature protocol for thermal/optical carbon analysis: maintaining consistency with a long-term database. J. Air Waste Manag. Assoc. 57, 1014–1023.

Dockery, D.W., Pope, C.A., 1994. Acute respiratory effects of particulate air pollution. Annu. Rev. Public Health 15, 107–132.

Engling, G., Carrico, C.M., Kreidenweis, S.M., Collett Jr., J.L., Day, D.E., Malm, W.C., Lincoln, E., Hao, W.M., Iinuma, Y., Herrmann, H., 2006. Determination of levoglucosan in biomass combustion aerosol by high performance anion exchange chromatography with pulsed amperometric detection. Atmos. Environ. 40, S299–S311.

Engling, G., Lee, J.J., Tsai, Y.W., Lung, S.C.C., Chou, C.C.K., Chan, C.Y., 2009. Size-resolved anhydrosugar composition in smoke aerosol from controlled field burning of rice straw. Aerosol Sci. Technol. 43 (7), 662–672.

Engling, G., Lee, J.J., Sie, H.J., Wu, Y.C., Pole, I.Y., 2012. Anhydrosugar characteristics in biomass smoke aerosol — case study of environmental influence on particle-size of rice straw burning aerosol. J. Aerosol Sci. http://dx.doi.org/10.1016/j.jaerosci.2012.10.001.

Gao, Y., Arimoto, R., Duce, R.A., Lee, D.S., Zhou, M.Y., 1992. Input of atmospheric trace elements and mineral matter to the Yellow Sea during the spring of a low-dust year. J. Geophys. Res. 97, 3767–3777.

Hays, M.D., Fine, P.M., Geron, C.D., Kleeman, M.J., Gullett, B.K., 2005. Opening burning of agricultural biomass: physical and chemical properties of particle-phase emissions. Atmos. Environ. 39, 6747–6764.

He, K.B., Yang, F.M., Ma, Y.L., Zhang, Q., Yao, X.H., Chan, C.K., Cadle, S., Chan, T., Mulawa, P., 2001. The characteristics of $PM_{2.5}$ in Beijing, China. Atmos. Environ. 35, 4959–4970.

Hennigan, C.J., Miracolo, M.A., Engelhart, G.J., May, A.A., Presto, A.A., Lee, T., Sullivan, A.P., McMeeking, G.R., Coe, H., Wold, C.E., Hao, W.-M., Gilman, J.B., Kuster, W.C., de Gouw, J., Schichtel, B.A., Collett Jr., J.L., Kreidenweis, S.M., Robinson, A.L., 2011. Chemical and physical transformations of organic aerosol from the photo-oxidation of open biomass burning emissions in an environmental chamber. Atmos. Chem. Phys. 11, 7669–7686.

Hennigan, C.J., Westervelt, M.W., Riipinen, I., Engelhart, G.J., Lee, T., Collett Jr., J.L., Pandis, S.N., Adams, P.J., Robinson, A.L., 2012. New particle formation and growth in biomass burning plumes: an important source of cloud condensation nuclei. J. Geophys. Res. 39, L09805. http://dx.doi.org/10.1029/2012GL050930.

Ho, K.F., Lee, S.C., Chan, C.K., Yu, J.C., Chow, J.C., Yao, X.H., 2003. Characterization of chemical species in $PM_{2.5}$ and PM_{10} aerosols in Hong Kong. Atmos. Environ. 37, 31–39.

Hu, M., Wu, Z.J., Slanina, J., Lin, P., Liu, S., Zeng, L.M., 2008. Acidic gases, ammonia and water-soluble ions in $PM_{2.5}$ at a coastal site in the Pearl River Delta, China. Atmos. Environ. 42, 6310–6320.

Hueglin, C., Gehrig, R., Baltensperger, U., Gysel, M., Monn, C., Vonmont, H., 2005. Chemical characterisation of $PM_{2.5}$, PM_{10} and coarse particles at urban, near-city and rural sites in Switzerland. Atmos. Environ. 39, 637–651.

Iinuma, Y., Brüggemann, E., Gnauk, T., Müller, K., Andreae, M.O., Helas, G., Parmar, R., Herrmann, H., 2007. Source characterization of biomass burning particles: the combustion of selected European conifers, African hardwood, savanna grass, and German and Indonesian peat. J. Geophys. Res. 112, D08209. http://dx.doi.org/10.1029/2006JD007120.

Iinuma, Y., Engling, G., Puxbaum, H., Herrmann, H., 2009. A highly resolved anion-exchange chromatographic method for determination of saccharidic tracers for biomass combustion and primary bio-particles in atmospheric aerosol. Atmos. Environ. 43, 1367–1371.

IMPROVE Report V, 2011. Spatial and seasonal patterns and temporal variability of haze and its constituents in the United States. Interagency Monitoring of Protected Visual Environments. Colorado State University.

Jacob, D.J., Winner, D.A., 2009. Effect of climate change on air quality. Atmos. Environ. 43, 51–63.

Kaufman, Y.J., Tanré, D., Boucher, O., 2002. A satellite view of aerosols in the climate system. Nature 419 (6903), 215–223.

Kondo, Y., Miyazaki, Y., Takegawa, N., Miyakawa, T., Weber, R.J., Jimenez, J.L., Zhang, Q., Worsnop, D.R., 2007. Oxygenated and water-soluble organic aerosols in Tokyo. J. Geophys. Res. 112, D01203. http://dx.doi.org/10.1029/2006JD007056.

Kumagai, K., Iijima, A., Tago, H., Tomioka, A., Kozawa, K., Sakamoto, K., 2009. Seasonal characteristics of water-soluble organic carbon in atmospheric particles in the inland Kanto plain, Japan. Atmos. Environ. 43, 3345–3351.

Kundu, S., Kawamura, K., Andreae, T.W., Hoffer, A., Andreae, M.O., 2010. Diurnal variation in the water-soluble inorganic ions, organic carbon and isotopic compositions of total carbon and nitrogen in biomass burning aerosols from the LBA-SMOCC campaign in Rondônia, Brazil. Aerosol Sci. 41, 118–133.

Laden, F., Neas, L.M., Dockery, D.W., Schwartz, J., 2000. Association of fine particulate matter from different sources with daily mortality in six U.S. Cities. Environ. Heal. Perspect. 108 (10), 941–947.

Lee, H.S., Kang, B.W., 2001. Chemical characteristics of principal $PM_{2.5}$ species in Chongju, South Korea. Atmos. Environ. 35, 739–746.

Lin, J.J., 2002. Characterization of the major chemical species in $PM_{2.5}$ in the Kaohsiung City, Taiwan. Atmos. Environ. 36, 1911–1920.

Lonati, G., Giugliano, M., Butelli, P., Romele, L., Tardivo, R., 2005. Major chemical components of $PM_{2.5}$ in Milan (Italy). Atmos. Environ. 39, 1925–1934.

Lowenthal, D.H., Kumar, N., 2005. Variation of mass scattering efficiencies in IMPROVE. J. Air Waste Manag. Assoc. 54, 926–934.

Mahowald, N.M., Dufresne, J., 2004. Sensitivity of TOMS aerosol index to boundary layer height: implications for detection of mineral aerosol sources. J. Geophys. Res. 31, L03103. http://dx.doi.org/10.1029/2003GL018865.

Maxwell-Meier, K., Weber, R., Song, C., Orsini, D., Ma, Y., 2004. Inorganic composition of fine particles in mixed mineral dust-pollution plumes observed from airborne measurements during ACE-Asia. J. Geophys. Res. 109, D19S07. http://dx.doi.org/10.1029/2003JD004464.

McMurry, P.H., 2000. A review of atmospheric aerosol measurements. Atmos. Environ. 34 (12–14), 1959–1999.

Minguillón, M.C., Perron, N., Querol, X., Szidat, S., Fahrni, S.M., Alastuey, A., Jimenez, J.L., Mohr, C., Ortega, A.M., Day, D.A., Lanz, V.A., Wacker, L., Reche, C., Cusack, M., Amato, F., Kiss, G., Hoffer, A., Decesari, S., Moretti, F., Hillamo, R., Teinilä, K., Seco, R., Peñuelas, J., Metzger, A., Schallhart, S., Müller, M., Hansel, A., Burkhart, J.F., Baltensperger, U., Prévôt, A.S.H., 2011. Fossil versus contemporary sources of fine elemental and organic carbonaceous particulate matter during the DAURE campaign in Northeast Spain. Atmos. Chem. Phys. 11, 12,067–12,084.

Na, K., Cocker III, D.R., 2009. Characterization and source identification of trace elements in $PM_{2.5}$ from Mira Loma, Southern California. Atmos. Res. 93, 793–800.

Norris, G., Vedantham, R., Wade, K., Brown, S., Prouty, J., Foley, C., 2008. EPA Positive Matrix Factorization (PMF) 3.0 Fundamentals & User Guide. U.S. Environmental Protection Agency, Office of Research and Development, Washington, DC.

Pitchford, M.L., Malm, W.C., Schichtel, B.A., et al., 2007. Revised formula for estimating light extinction from IMPROVE particle speciation data. J. Air Waste Manag. Assoc. 57, 1326–1336.

Polissar, A.V., Hopke, P.K., Paatero, P., Malm, W.C., Sisler, J.F., 1998. Atmospheric aerosol over Alaska: 2. Elemental composition and sources. J. Geophys. Res. 103 (D15), 19,045–19,057.

Pope, C.A., Dockery, D.W., 2006. Health effects of fine particulate air pollution: lines that connect. J. Air Waste Manag. Assoc. 56, 709–742.

Putaud, J.P., Raes, F., Dingenen, R.V., Brüggemann, E., Facchini, M.C., Decesari, S., Fuzzi, S., Gehrig, R., Hüglin, C., Laj, P., Lorbeer, G., Maenhaut, W., Mihalopoulos, N., Müller, K., Querol, X., Rodriguez, S., Schneider, J., Spindler, G., Brink, H., Tørseth, K., Wiedensohler, A., 2004. A European aerosol phenomenology—2: chemical characteristics of particulate matter at kerbside, urban, rural and background sites in Europe. Atmos. Environ. 38, 2579–2595.

Querol, X., Alastuey, A., Viana, M.M., Rodriguez, S., Artiñano, B., Salvador, P., Garcia do Santos, S., Fernandez Pater, R., Ruiz, C.R., de la Rosa, J., Sanchez de la Campa, A., Menedez, M., Gil, J.I., 2004. Speciation and origin of PM_{10} and $PM_{2.5}$ in Spain. J. Aerosol Sci. 35, 1151–1172.

Ram, K., Sarin, M.M., 2011. Day–night variability of EC, OC, WSOC and inorganic ions in urban environment of Indo-Gangetic Plain: implications to secondary aerosol formation. Atmos. Environ. 45, 460–468.

Reff, A., Eberly, S.I., Bhave, P.V., 2007. Receptor modeling of ambient particulate matter data using positive matrix factorization: review of existing methods. J. Air Waste Manag. Assoc. 57 (2), 146–154.

Rengarajan, R., Sudheer, A.K., Sarin, M.M., 2011. Wintertime $PM_{2.5}$ and PM_{10} carbonaceous and inorganic constituents from urban site in western India. Atmos. Res. 102, 420–431.

Robinson, A.L., Donahue, N.M., Shrivastava, M.K., Weitkamp, E.A., Sage, A.M., Grieshop, A.P., Lane, T.E., Pierce, J.R., Pandis, S.N., 2007. Rethinking organic aerosols: semivolatile emissions and photochemical aging. Science 315, 1259–1262.

Ryu, S.Y., Kim, J.E., Zhuanshi, H., Kim, Y.J., Kang, G.U., 2004. Chemical composition of post-harvest biomass burning aerosols in Gwangju, Korea. J. Air Waste Manag. Assoc. 54, 1124–1137.

Ryu, S.Y., Kwon, B.G., Kim, Y.J., Kim, H.H., Chun, K.J., 2007. Characteristics of biomass burning aerosol and its impact on regional air quality in the summer of 2003 at Gwangju, Korea. Atmos. Res. 84, 362–373.

Samet, J.M., Dominici, F., Curriero, F.C., Coursac, I., Zeger, S.L., 2000. Fine particulate air pollution and mortality in U.S. cities, 1987–1994. N. Engl. J. Med. 343 (24), 1742–1749.

Schwarz, J., Chi, X., Maenhaut, W., Civiš, M., Hovorka, J., Smolík, J., 2008. Elemental and organic carbon in atmospheric aerosols at downtown and suburban sites in Prague. Atmos. Res. 90, 287–302.

Shen, Z.X., Cao, J.J., Arimoto, R., Zhang, R.J., Jie, D.M., Liu, S.X., 2007. Chemical composition and source characterization of spring aerosol over Horqin sand land in northeastern China. J. Geophys. Res. 112, D14315. http://dx.doi.org/10.1029/2006JD007991.

Shen, Z.X., Cao, J.J., Arimoto, R., Han, Z.W., Zhang, R.J., Han, Y.M., Liu, S.X., Okuda, T., Nakao, S., Tanaka, S., 2009. Ionic composition of TSP and $PM_{2.5}$ during dust storms and air pollution episodes at Xi'an, China. Atmos. Environ. 43, 2911–2918.

Sisler, J.F., Malm, W.C., 2000. Interpretation of trends of PM$_{2.5}$ and reconstructed visibility from the IMPROVE network. J. Air Waste Manag. Assoc. 50, 775–789.

Solomon, P.A., Hopke, P.K., Froines, J., Scheffe, R., 2008. Key scientific findings and policy- and health-relevant insights from the U.S. Environmental Protection Agency's particulate matter supersites program and related studies: an integration and synthesis of results. J. Air Waste Manag. Assoc. 58 (13 Suppl.), S3–S92.

Sullivan, A.P., Holden, A.S., Patterson, L.A., McMeeking, G.R., Kreidenweis, S.M., Malm, W.C., Hao, W.M., Wold, C.E., Collett, J.L., 2008. A method for smoke marker measurements and its potential application for determining the contribution of biomass burning from wildfires and prescribed fires to ambient PM$_{2.5}$ organic carbon. J. Geophys. Res. 113, D22302. http://dx.doi.org/10.1029/2008JD010216.

Tao, J., Ho, K.F., Chen, L.G., Zhu, L.H., Han, J.L., Xu, Z.C., 2009. Effect of chemical composition of PM$_{2.5}$ on visibility in Guangzhou, China, 2007 spring. Particuology 7, 68–75.

Taylor, S.R., McLennan, S.M., 1995. The geochemical evolution of the continental crust. Rev. Geophys. 33, 241–265.

Turpin, B.J., Huntzicker, J.J., 1995. Identification of secondary aerosol episodes and quantification of primary and secondary organic aerosol concentrations during SCAQS. Atmos. Environ. 29, 3527–3544.

Veysseyre, A., Moutard, K., Ferrari, C., Van de Velde, K., Barbante, C., Cozzi, G., Capodaglio, G., Boutron, C., 2001. Heavy metals in fresh snow collected at different altitudes in the Chamonix and Maurienne valleys, French Alps: initial results. Atmos. Environ. 35, 415–425.

Wang, G., Li, J., Cheng, C., Hu, S., Xie, M., Gao, S., Zhou, B., Dai, W., Cao, J., An, Z., 2011. Observation of atmospheric aerosols at Mt. Hua and Mt. Tai in central and east China during spring 2009—part 1: EC, OC and inorganic ions. Atmos. Chem. Phys. 11, 4221–4235.

Watson, J.G., 2002. Visibility: science and regulation. J. Air Waste Manag. Assoc. 52, 628–713.

Watson, J.G., Chow, J.C., Houck, J.E., 2001. PM$_{2.5}$ chemical source profiles for vehicle exhaust, vegetative burning, geological material, and coal burning in Northwestern Colorado during 1995. Chemosphere 43, 1141–1151.

Wedepohl, H.K., 1995. The composition of the continental crust. Geochim. Cosmochim. Acta 59, 1217–1232.

Wei, F., Teng, E., Wu, G., Hu, W., Willson, W.E., Chapman, R.S., Pau, J.C., Zhang, J., 1999. Ambient concentrations and elemental compositions of PM$_{10}$ and PM$_{2.5}$ in four Chinese cities. Environ. Sci. Technol. 33 (23), 4188–4193.

Xu, J., Bergin, M.H., Greenwald, R., Schauer, J.J., Shafer, M.M., Jaffrezo, J.L., Aymoz, G., 2004. Aerosol chemical, physical, and radiative characteristics near a desert source region of northwest China during ACE-Asia. J. Geophys. Res. 109, D19S03. http://dx.doi.org/10.1029/2003JD004239.

Xu, H.M., Cao, J.J., Ho, K.F., Ding, H., Han, Y.M., Wang, G.H., Chow, J.C., Watson, J.G., Khol, S.D., Qiang, J., Li, W.T., 2012. Lead concentrations in fine particulate matter after the phasing out of leaded gasoline in Xi'an, China. Atmos. Environ. 46, 217–224.

Yang, F., Tan, J., Zhao, Q., Du, Z., He, K., Ma, Y., Duan, F., Chen, G., Zhao, Q., 2011. Characteristics of PM$_{2.5}$ speciation in representative megacities and across China. Atmos. Chem. Phys. 11, 5207–5219.

Yang, Y., Chan, C., Tao, J., Lin, M., Engling, G., Zhang, Z., Zhang, T., Su, L., 2012. Observation of elevated fungal tracers due to biomass burning in the Sichuan Basin at Chengdu City, China. Sci. Total. Environ. 431, 68–77.

Ye, B.M., Ji, X.L., Yang, H.Z., Yao, X.H., Chan, C.K., Cadle, S.H., Chan, T., Mulawa, P.A., 2003. Concentration and chemical composition of PM$_{2.5}$ in Shanghai for a 1-year period. Atmos. Environ. 37, 499–510.

Zhang, R.J., Wang, M.X., Xia, X.A., 2002. Chemical composition of aerosol in winter/spring in Beijing. J. Environ. Sci. 14 (1), 7–11.

Zhang, R.J., Wang, M.X., Zhang, X.Y., Zhu, G.H., 2003a. Analysis on the chemical and physical properties of particles in a dust storm in spring in Beijing. Powder Technol. 137, 77–82.

Zhang, X.Y., Gong, S.L., Shen, Z.X., Mei, F.M., Xi, X.X., Liu, L.C., Zhou, Z.J., Wang, D., Wang, Y.Q., Cheng, Y., 2003b. Characterization of soil dust aerosol in China and its transport and distribution during 2001 ACE-Asia: 1. Network observations. J. Geophys. Res. 108, 4261. http://dx.doi.org/10.1029/2002JD002632.

Zhang, R.J., Cao, J.J., Lee, S.C., Shen, Z.X., Ho, K.F., 2007. Carbonaceous aerosols in PM$_{10}$ and pollution gases in winter in Beijing. J. Environ. Sci. 19, 564–571.

Zhang, T., Claeys, M., Cachier, H., Dong, S.P., Wamg, W., Maenhaut, W., Liu, X.D., 2008. Identification and estimation of the biomass burning contribution to Beijing aerosol using levoglucosan as a molecular marker. Atmos. Environ. 42, 7013–7021.

Zhang, Z.S., Engling, G., Lin, C.Y., Chou, C.C.K., Lung, S.C.C., Chang, S.Y., Fan, S.J., Chan, C.Y., Zhang, Y.H., 2010. Chemical speciation, transport and contribution of biomass burning smoke to ambient aerosol in Guangzhou, a mega city of China. Atmos. Environ. 44, 3187–3195.

Zhang, T., Cao, J.J., Tie, X.X., Shen, Z.X., Liu, S.X., Ding, H., Han, Y.M., Wang, G.H., Ho, K.F., Qiang, J., Li, W.T., 2011. Water-soluble ions in atmospheric aerosols measured in Xi'an, China: seasonal variations and sources. Atmos. Res. 102, 110–119.

Zhang, R.J., Tao, J., Ho, K.F., Shen, Z., Cao, J., Liu, S., Zhang, L., Lee, S.C., 2012. Characterization of springtime atmospheric organic and elemental carbon of PM$_{2.5}$ in a typical semi-arid area of Northeastern China. Aerosol Air Qual. Res. 12, 792–802.

Zhao, Q., He, K., Rahn, K.A., Ma, Y., Jia, Y., Yang, F., Duan, F., Lei, Y., Chen, G., Cheng, Y., Liu, H., Wang, S., 2010. Dust storms come to Central and Southwestern China, too: implications from a major dust event in Chongqing. Atmos. Chem. Phys. 10, 2615–2630.